

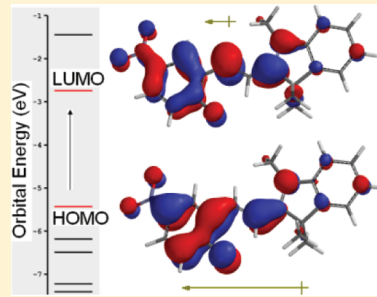
Thermosolvatochromism of Nitrospiropyran and Merocyanine Free and Bound to Cyclodextrin

Kathryn Burke, Caterina Riccardi, and Thandi Buthelezi*

Department of Chemistry, Wheaton College, Norton, Massachusetts 02766, United States

S Supporting Information

ABSTRACT: The thermosolvatochromism of nitrospiropyran free and bound to cyclodextrin was studied in dimethylsulfoxide (DMSO)–water binary solvent systems. Spiropyran was interconverted to merocyanine by heating the sample to 55 °C. The merocyanine (MC) was converted back to spirocyclic (SP) either by cooling the sample to room temperature or irradiating the sample with a visible light emitting diode. Steady state absorption spectra of SP and MC samples in the free state and bound to cyclodextrin were obtained in several DMSO–water binary solutions. Emission spectra of MC both free and cyclodextrin-bound were also acquired. Blue-shifted absorption and emission spectra of the studied molecules with increasing solvent polarity suggest that the dipole moments of free and bound merocyanines are higher in the ground state compared to the excited state. Merocyanine dipole moments in the ground and excited states were determined using thermosolvatochromism measurements and the Lippert–Mataga, Bakhshiev, and Kawski–Chamma–Viallet polarity functions. A large change in the dipole moment (ca. 16 D) of the merocyanine in aqueous DMSO was obtained upon electronic excitation, $S_1 \leftarrow S_0$. Analysis of the merocyanine Stokes' shifts as a function of solvent polarity indicates that both general solvent effects and specific solvent effects are present in all systems studied. These findings reveal that merocyanine could be utilized as a polarity sensor for DMSO–water binary solutions.



INTRODUCTION

In this paper, we add to the small number of existing studies of merocyanine (MC) in binary aqueous solvents¹ by investigating the thermosolvatochromism of MC in the free state and bound to cyclodextrin in dimethylsulfoxide (DMSO)–water binary solvent systems, as a function of temperature, solvent polarity, and viscosity. In the past the aqueous–dimethylsulfoxide medium has been extensively studied because of its low toxicity, importance in biological systems, and drug delivery.^{2–7} During the past decade there has been an increasing interest in the thermosolvatochromism of merocyanines because of their potential applications in optical switches, temperature, and polarity sensors.^{1,8–12} Our investigation focused on measuring spectroscopically the color change of merocyanine in DMSO–water at 55 °C. The observed thermosolvatochromism is a characteristic property of MC in DMSO–water that could be used to estimate the temperature and/or polarity of a solution or its microenvironment. This characteristic property can contribute to the development of temperature sensors and/or polarity sensors.^{8–10}

Merocyanines are photochromic molecules, that is, they reversibly interconvert from spirocyclic (SP; closed-ring form) into merocyanine (open-ring form) in the presence and absence of ultraviolet light or heat. The ring-opening conversion of SP to MC causes a heterolytic cleavage of the C–O bond that shifts the absorption band of spirocyclic from the UV spectral range to the visible range in merocyanine (Figure 1) because of the increased conjugation in the system.^{11,12} In solution, the interconversion is solvent-polarity dependent which causes solvatochromism.^{8,12}

In neat solvents, SP converts to MC through irradiation by UV light ($\lambda = 365$ nm, 8 W mercury lamp). However, in

aqueous DMSO binary solvents, irradiation of SP with the same UV lamp did not produce a color change; this observation is in accord with a similar observation for SP–MC conversion in water–methanol binary media.¹ In our studies merocyanine was formed by heating a solvated sample of spirocyclic to 55 °C which yielded several isomers of merocyanine including the zwitterionic and quinoidal structures shown in Figure 1. The zwitterionic form is favored in the ground state (S_0) and more polar solvents, whereas the quinoidal form is favored in the first excited state (S_1) and less polar media. The general representation of merocyanines is D–R–A, where D is the electron donor (i.e., oxygen anion), R is the conjugation path, and A is the electron acceptor (i.e., nitrogen cation). Upon electronic excitation, the merocyanine zwitterionic form converts to its quinoidal structure via intramolecular charge transfer.¹³

We present here the steady state absorption studies of the bound and unbound spirocyclic host/guest complexes in aqueous DMSO binary solvents. In the host/guest complexes the guest molecule, MC or SP, is intercalated into the cavity of the host molecule, cyclodextrin. For the MC system, we present absorption and fluorescence spectra of the MC host/guest complexes unbound and bound to cyclodextrin in binary DMSO–water solvents. Fluorescence spectra of the solvents and SP systems alone were not acquired since these chromophores do not fluoresce in the UV–vis spectral range. The SP and MC host/guest

Received: August 20, 2011

Revised: November 17, 2011

Published: January 30, 2012

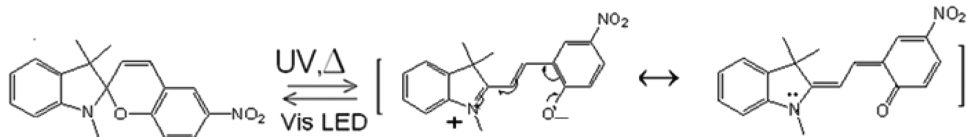


Figure 1. Spiropyran interconversion to merocyanine (zwitterionic and quinoidal) structures upon heating or UV light irradiation and the reverse reaction forming spiropyran via absorption of visible light following irradiation with a light emitting diode (LED).

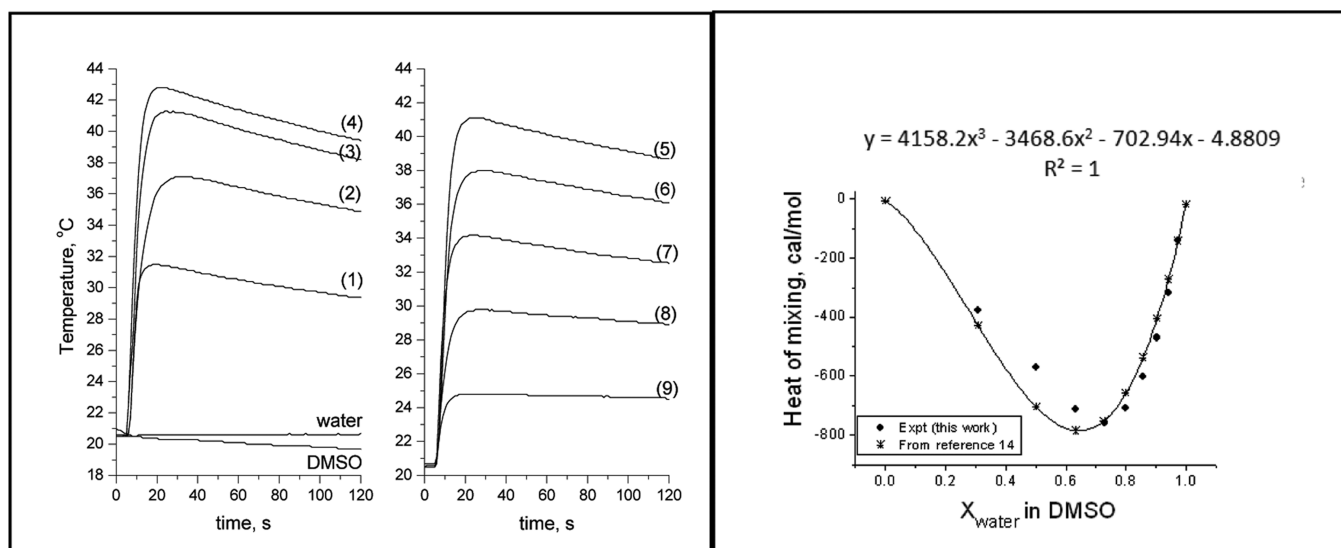


Figure 2. Temperature (left) and heat of mixing (right) changes for the DMSO–water system at room temperature. Numbers 1–9 correspond to added volume percent water of 10–90% in DMSO. The heat of mixing experimental values from ref 14 (asterisk symbols) were fitted to a cubic function (curve), and the diamond symbols are heat of mixing values that we estimated from $C_p \Delta T$.

complexes were bound to either gamma-cyclodextrin (γ -CD) or 2-hydroxypropyl-gamma-cyclodextrin (HP γ CD).

■ EXPERIMENTAL METHODS

The chemicals nitrospiropyran (1',3'-dihydro-1',3',3'-trimethyl-6-nitrospiro[2H-1-benzopyran-2,2'-(2H)-indole]), 2-hydroxypropyl- γ -cyclodextrin, γ -cyclodextrin, and the solvent DMSO were purchased from Sigma-Aldrich and used as received. Stock solutions of the spiropyran (1 mM) in DMSO and cyclodextrins (2 mM) in deionized water were prepared. Control solutions of DMSO–water without the chromophores were prepared by varying the volume of water from 0 to 9 mL while decreasing the volume of DMSO in a 10 mL volumetric flask. The Logger Pro temperature probe was used to measure changes in solution temperature upon mixing in a custom-built calorimeter. Absorption spectra of these solutions were acquired using an empty cuvette as a blank at ambient temperature.

For unbound spiropyran systems, ten solutions of fixed concentration of spiropyran (ca. 0.1 mM) in various binary DMSO–water solvents were prepared in 10 mL volumetric flasks, including one with neat DMSO as a solvent. Solutions were not made in pure water since SP is water insoluble. Media polarity was changed by varying the volume of water from 0 to 9 mL in each set of solutions. These aqueous DMSO solutions increased in polarity from the less polar pure DMSO solvent to the highly polar dimethylsulfoxide–water (1:9 v/v) and had dielectric constants varying from 48.68 to 77.02 at room temperature. For the bound spiropyran system, the concentration of SP was also kept constant at 0.1 mM and that of the cyclodextrin was held fixed at 0.2 mM in DMSO–water solutions of varying polarity.

Room temperature absorption spectra were recorded with an Agilent 8453 UV–vis photodiode array. Temperature-variable absorption spectra were taken from a Perkin-Elmer Lambda 750 UV/VIS/NIR spectrophotometer coupled with a Qpod 2e temperature-controlled sample compartment. Absorption titration experiments were conducted to confirm the cyclodextrin–spiropyran and cyclodextrin–merocyanine 1:1 complexation. Nonlinear least-squares analysis of the titration data is provided in the Supporting Information. Steady state fluorescence spectra were acquired from a temperature-adjustable PE LS55 spectrofluorimeter with a working temperature range of 20–60 °C. A Fisher Scientific Isotemp water bath was used to equilibrate samples at a specific temperature prior to the acquisition of absorption and fluorescence spectra. Molecular orbital energies and simulated UV–vis spectra of SP and MC were calculated on a Dell Precision M6500 workstation using SPARTAN'10 v1.0.1 software. Density functional theory (DFT) with the B3LYP functional and 6-31G* basis set was used to calculate the HOMO and LUMO energies for the spiropyran and merocyanine molecules in the gas phase.

■ RESULTS AND DISCUSSION

1. DMSO–Water Solutions in the Absence of a Chromophore. The mixing of DMSO and water at room temperature is exothermic and thermodynamically favored. The stronger DMSO–water intermolecular forces stabilize the media compared to individual DMSO solvent–solvent intermolecular forces. Figure 2 shows changes in temperature of the aqueous DMSO solutions upon mixing varying volumes of water with DMSO to a final volume of 10 mL at room temperature. In this study, we prepared solutions using volume

fraction of water and measured the change in temperature of the solution upon mixing. Enthalpies of mixing of DMSO–water as a function of the mole fraction of water have been reported.¹⁴ The water volume fractions were converted to mole fractions, and these values were used to estimate the molar heat of mixing for the DMSO and water system ($\Delta H_{\text{mix,molar}}$) according to the following expression

$$\begin{aligned} (\Delta H_{\text{mix,molar}}) &= x_{\text{water}} \Delta H_{\text{water,molar}} \\ &\quad + (1 - x_{\text{water}}) \Delta H_{\text{DMSO,molar}} \\ &= C_{\text{p,mix,molar}} \Delta T \end{aligned} \quad (1)$$

where $\Delta H_{\text{water,molar}}$ and $\Delta H_{\text{DMSO,molar}}$ are partial molar enthalpies of water and DMSO, respectively.

The literature experimental heat of mixing values¹⁴ were plotted as a function of the mole fraction of water, and the data points were fitted to a cubic expression (Figure 2). We used the derived expression to predict molar enthalpies of mixing for continuous mole fraction of water in DMSO. The predicted molar enthalpy of mixing ($\Delta H_{\text{mix,molar}}$) and the observed ΔT values were used to estimate the average molar heat capacity of the solutions ($C_{\text{p,mix,molar}}$) ca. 34 ± 8 cal/mol·K, assuming that the heat capacity is temperature independent. Figure 2 shows estimated heats of mixing (filled diamond symbols) using the average molar heat capacity and measured changes in temperature upon mixing DMSO and water solvents. The estimated heats of formation suggest that the heat capacity of the DMSO–water solution is temperature dependent for solutions with a mole fraction of water below 0.7 and is relatively temperature independent for solutions with water mole fraction greater than 0.7.

Absorption spectra of the binary aqueous DMSO solvents were recorded at room temperature and used to construct a Beer's plot, Figure 3, at the water absorbance at 975 nm. The linearity of the Beer's plot ($R^2 = 0.99$, $\epsilon_{975} = 0.0345 \text{ M}^{-1} \text{ cm}^{-1}$) suggests that Beer–Lambert law is a reliable predictor of water concentration in the aqueous–DMSO binary mixtures. As expected the DMSO absorbances at 900, 1010, and 1060 nm

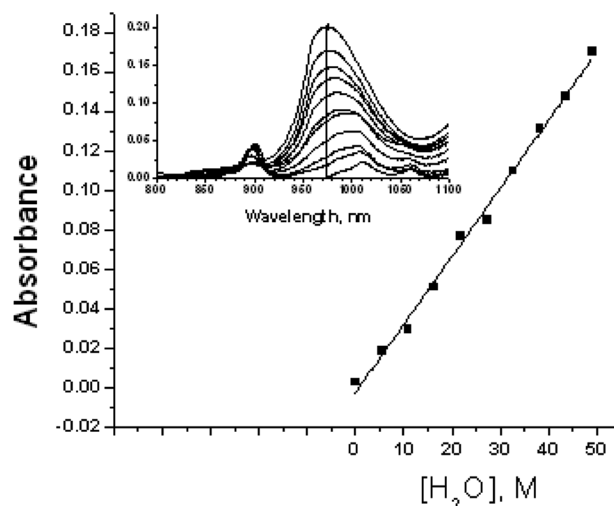


Figure 3. Beer's plot of water in DMSO at 975 nm and $T = 25^\circ\text{C}$. The insert shows absorption spectra of increasing concentrations of water from zero (pure DMSO solvent) to pure water, which is equivalent to 0.0017 mol of water in a 10 mL volumetric flask. The upward arrow at 975 nm indicates the direction of increasing water concentration.

decreased as the water content of the solution increased since the total solution volume was kept constant at 10 mL.

2. Spiropyran Free and Bound to Cyclodextrin in Binary DMSO–Water Solutions. The maximum wavelengths of absorption of unbound spiropyran and bound to cyclodextrin are constant for all solutions at ca. 350 nm (Figure 4). Data for cyclodextrin bound spirocyclics are not shown. However, the absorbance intensities of these molecules decrease with increasing solvent polarity. This observation is not surprising since SP in the ground state is relatively nonpolar and, therefore, is not expected to have significant interactions with polar solvents. In fact as the polarity of the DMSO–water solvents increases, the solubility of spiropyran decreases which supports the decrease in absorbance values of the chromophore. Moreover, when dissolving SP in aqueous–DMSO binary solvents,

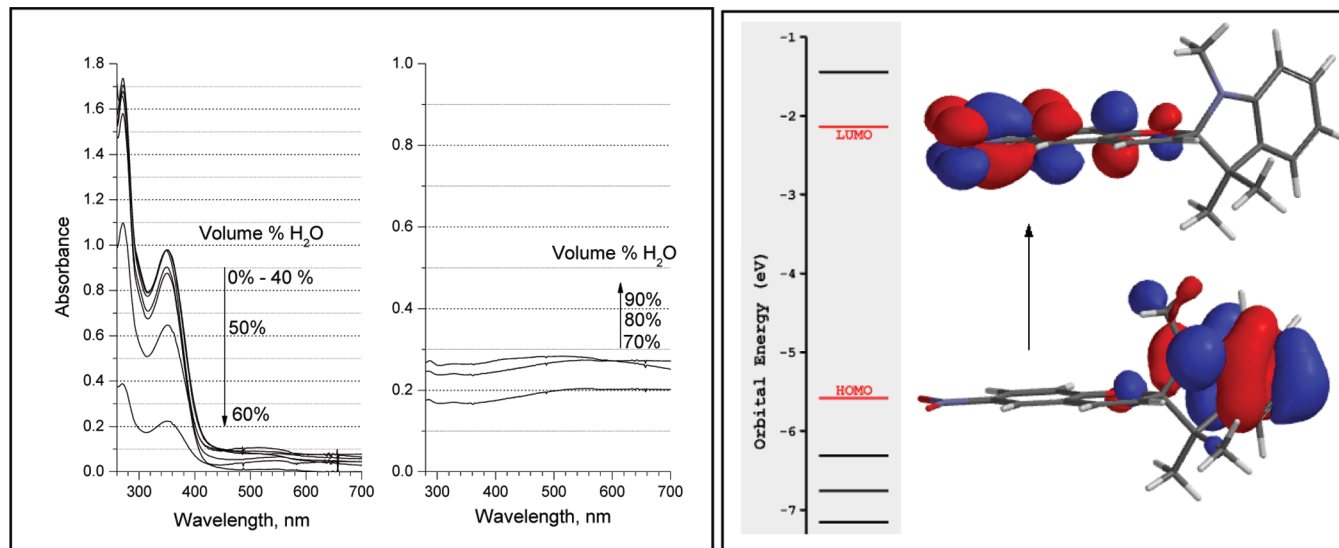


Figure 4. Absorption spectra of free SP in aqueous DMSO solutions (0–90 vol % water) at room temperature. Molecular orbitals of SP in the gas phase (right) calculated from the DFT B3LYP 6-31G* basis set show the intramolecular charge transfer from the ground state (HOMO) to the first excited state (LUMO).

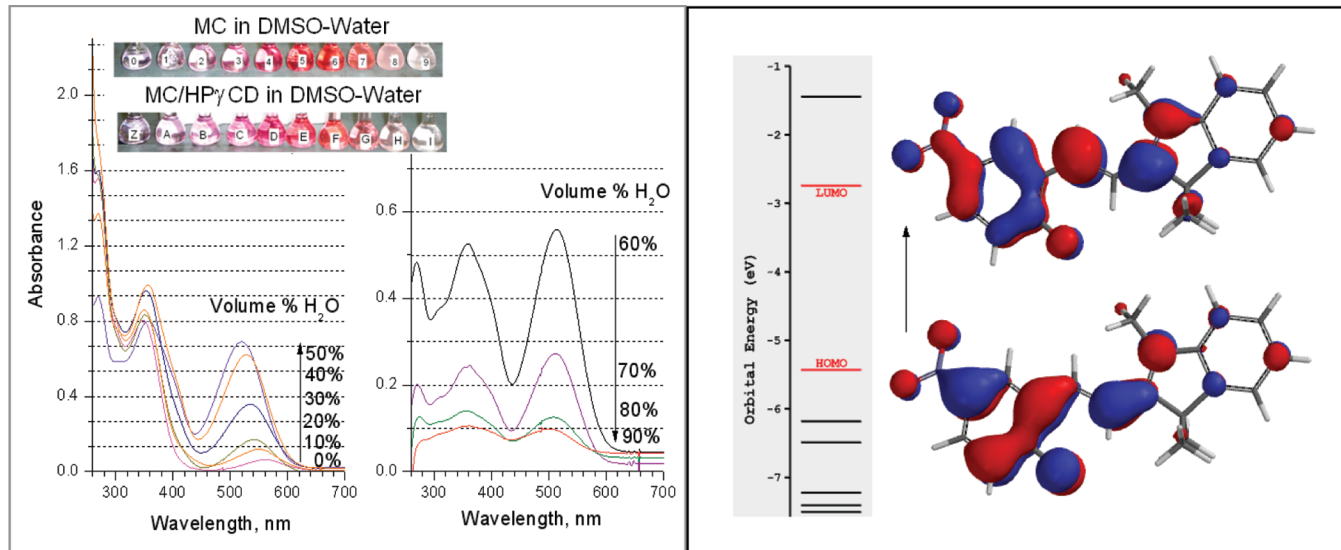


Figure 5. Absorption spectra of HP γ CD-MC in DMSO–water solutions (v/v): (Z) 10/0, (A) 9/1, (B) 8/2, (C) 7/3, (D) 6/4, (E) 5/5, (F) 4/6, (G) 3/7, (H) 2/8, and (I) 1/9 at 55 °C. Molecular orbitals of MC in the gas phase (right) calculated from DFT B3LYP show the intramolecular charge transfer from the ground state (HOMO) to the first excited state (LUMO). The orbitals are delocalized over the whole molecule.

a precipitate forms in solvents of higher water concentration (that is, for a water volume of 70% or higher) as evidenced by lack of an absorbance peak at 350 nm, Figure 4. In contrast, we observed a continuum throughout the range 260–700 nm in the absorption spectra of spiropyran solutions with water volume \geq 70%. Observation of a continuum, instead of a peak, is common for cloudy solutions with precipitate. However, upon heating or addition of cyclodextrins (γ -CD or HP γ CD), the solubility of SP in solutions of higher polarity improved, that is, solutions became clear.

The quantum mechanical DFT with B3LYP functional and 6-31G* calculated highest occupied molecular orbital–lowest unoccupied molecular orbital (HOMO–LUMO) transition for the free spiropyran in the gas phase is ca. 360 nm and compares favorably with the experimental value of 350 nm in aqueous DMSO medium. The experimental dipole moments of spiropyran are 4.2 and 18.5 D in dioxane for the ground and excited state, respectively.¹² Upon photoexcitation, spiropyran experiences a large change in dipole moment (14.3 D) evidenced by the intramolecular charge transfer that is shown by the localized HOMO and LUMO transition (Figure 4). Unfortunately, SP does not fluoresce in the UV–vis spectral range; therefore, we were not able to measure solvent effects in the excited state for this system. However, SP phosphoresces although the quantum yield for the SP phosphorescence in DMSO–water is very low.

3. MC Free and Bound to Cyclodextrin in DMSO–Water Solutions. In contrast to the SP system, the MC absorbance maximum wavelengths shift to lower wavelengths (higher energies) as a function of solvent polarity. Moreover, the measured absorbance intensities of bound and unbound MC scales with the solvent polarity for DMSO solutions with water content from 0–50% by volume (Figure 5). This trend switches at higher water concentrations; for DMSO–water solutions that contain \geq 60% water by volume, the absorbance intensities of MC decrease as the solvent polarity increases. This observation may result from a decrease in the solubility of SP as the water content increases directly affecting the amount of MC in solution. Specifically, the absorption maximum of spiropyran at 350 nm is at 0.8 or higher for solutions with water

content between 0 and 50%. However, for the binary DMSO–water solution with water content between 60 and 90%, the SP absorbance at 350 nm decreases from 0.5 to 0.1. Other contributing factors may be from unfavorable Franck–Condon factors, increased hydrogen bonding between the solvent and chromophores, and/or formation of aggregates.

The absorption and fluorescence spectra (Figures 5 and 6) of merocyanine free and bound to cyclodextrin are solvent

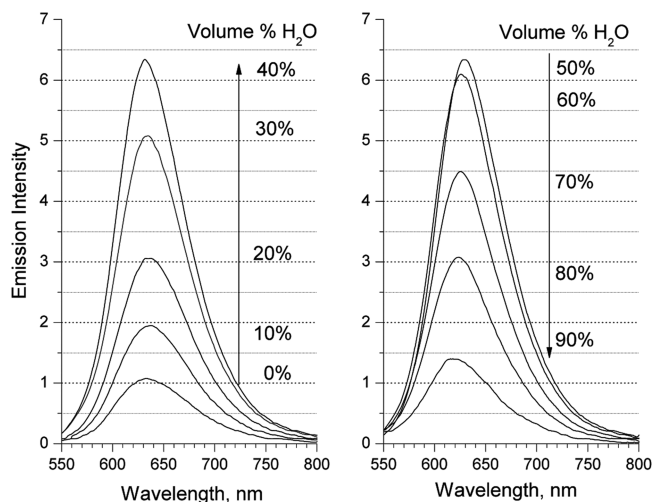


Figure 6. Emission spectra of HP γ CD–MC in DMSO–water solutions ranging from 0% water, that is, pure DMSO, to 90% by volume water in DMSO at 55 °C. The excitation wavelength is at 520 nm.

dependent, suggesting that MC could serve as a polarity sensor. We analyzed solvent effects on the MC HOMO–LUMO transition by examining the Stokes' shifts according to the Lippert–Mataga,^{15,16} Bakhshiev,¹⁷ and Kawski–Chamma–Viallet^{18–20} polarity functions below:

$$\Delta\nu_{\text{Stokes}} = (\tilde{\nu}_a - \tilde{\nu}_f) = m_1 \Delta f_{\text{Lippert–Mataga}} + \text{constant} \quad (2)$$

Table 1. Spectroscopic Data with Calculated Orientation Polarizabilities, Stokes' shifts, and Quantum Yield

solute	soln ^a	vol % H ₂ O	ϵ^b	n_D^b	$\Delta f(LM)$	$\Delta f(B)$	$\Delta f(KCV)$	Stokes shift ($\Delta \tilde{\nu}/\text{cm}^{-1}$)	quantum yield
MC	0	0	48.879	1.478	0.264	0.844	0.745	2059	0.031
	1	10	58.089	1.432	0.281	0.870	0.728	2417	0.040
	2	20	63.842	1.404	0.292	0.883	0.716	2721	0.042
	3	30	67.777	1.385	0.299	0.892	0.708	2974	0.033
	4	40	70.638	1.371	0.305	0.898	0.701	3175	0.020
	5	50	72.812	1.360	0.309	0.902	0.696	3381	0.014
	6	60	74.521	1.351	0.312	0.906	0.692	3519	0.013
	7	70	75.898	1.345	0.315	0.908	0.689	3659	0.023
	8	80	77.032	1.339	0.317	0.910	0.686	3843	0.028
	9	90	77.982	1.334	0.319	0.912	0.684	3899	0.021
solute	soln ^a	vol % H ₂ O	ϵ^b	n_D^b	$\Delta f(LM)$	$\Delta f(B)$	$\Delta f(KCV)$	Stokes shift ($\Delta \tilde{\nu}/\text{cm}^{-1}$)	quantum yield
γ CD-MC	Z	0	48.879	1.478	0.264	0.844	0.745	2003	0.034
	A	10	58.089	1.432	0.281	0.870	0.728	2195	0.045
	B	20	63.842	1.404	0.292	0.883	0.716	2662	0.054
	C	30	67.777	1.385	0.299	0.892	0.708	2869	0.041
	D	40	70.638	1.371	0.305	0.898	0.701	2668	0.022
	E	50	72.812	1.360	0.309	0.902	0.696	2768	0.017
	F	60	74.521	1.351	0.312	0.906	0.692	2976	0.022
	G	70	75.898	1.345	0.315	0.908	0.689	3416	0.038
	H	80	77.032	1.339	0.317	0.910	0.686	3479	0.045
	I	90	77.982	1.334	0.319	0.912	0.684	3543	0.024
solute	soln ^a	vol % H ₂ O	ϵ^b	n_D^b	$\Delta f(LM)$	$\Delta f(B)$	$\Delta f(KCV)$	Stokes shift ($\Delta \tilde{\nu}/\text{cm}^{-1}$)	quantum yield
HP γ CD-MC	Z	0	48.879	1.478	0.264	0.844	0.745	1901	0.037
	A	10	58.089	1.432	0.281	0.870	0.728	2188	0.057
	B	20	63.842	1.404	0.292	0.883	0.716	2551	0.048
	C	30	67.777	1.385	0.299	0.892	0.708	2904	0.052
	D	40	70.638	1.371	0.305	0.898	0.701	3149	0.041
	E	50	72.812	1.360	0.309	0.902	0.696	3342	0.034
	F	60	74.521	1.351	0.312	0.906	0.692	3480	0.035
	G	70	75.898	1.345	0.315	0.908	0.689	3569	0.025
	H	80	77.032	1.339	0.317	0.910	0.686	3634	0.026
	I	90	77.982	1.334	0.319	0.912	0.684	3753	0.016

^aFor the MC system solution, numbers 0–9 indicate the amount (mL) of water added to DMSO in each 10 mL volumetric flask. Analogous solutions were prepared for solutions z–i and Z–I with the upper and lower case z indicating systems in neat DMSO. Samples a and A have 1 mL of water added and I and I have 9 mL of water added to DMSO. ^bValues taken from ref 14.

$$\Delta v_{\text{Stokes}} = (\tilde{\nu}_a - \tilde{\nu}_f) = m_2 \Delta f_{\text{Bakhshiev}} + \text{constant} \quad (3)$$

$$\left(\frac{\tilde{\nu}_a + \tilde{\nu}_f}{2} \right) = m_3 \Delta f_{\text{Kawski-Chamma-Viallet}} + \text{constant} \quad (4)$$

where $\tilde{\nu}_a$ and $\tilde{\nu}_f$ are absorption and fluorescence maximum energies in wavenumbers, m represents the slopes where

$$m_1 = m_2 = \frac{2(\mu_e - \mu_g)^2}{hca^3} \quad (5)$$

and

$$m_3 = \frac{2(\mu_e^2 - \mu_g^2)}{hca^3} \quad (6)$$

μ_e and μ_g are the electronic excited and ground state dipole moments (esu·cm), h is Planck's constant (erg·s), c is the speed of light in a vacuum (cm/s), a is the cavity radius of the fluorophore—merocyanine—(cm). Knowing the change in dipole moment upon electronic excitation, from the slopes of the Lippert-Mataga, Bakhshiev, and Kawski-Chamma-Viallet plots, and the ratio of the dipole moments, from eq 7 below,

allows for the determination of the ground and excited state dipole moments.

$$\frac{\mu_e}{\mu_g} = \frac{|m_1 + m_2|}{|m_2 - m_1|} \quad (7)$$

The polarizability reorientation functions, Δf , given in Table 1 were calculated by using eqs 8–10:

$$\begin{aligned} \Delta f_{\text{Kawski-Chamma-Viallet}} &= \left[\frac{2n^2 + 1}{2(n^2 + 2)} \left(\frac{\varepsilon - 1}{\varepsilon + 2} - \frac{n^2 - 1}{n^2 + 1} \right) - \frac{3(n^4 - 1)}{2(n^2 + 2)^2} \right] \\ &= \left[\frac{2n^2 + 1}{2(n^2 + 2)} \left(\frac{\varepsilon - 1}{\varepsilon + 2} - \frac{n^2 - 1}{n^2 + 1} \right) - \frac{3(n^4 - 1)}{2(n^2 + 2)^2} \right] \end{aligned} \quad (8)$$

$$\Delta f_{\text{Lippert-Mataga}} = \frac{\varepsilon - 1}{2\varepsilon + 1} - \frac{n^2 - 1}{2n^2 + 1} \quad (9)$$

$$\Delta f_{\text{Bakhshiev}} = \frac{2n^2 + 1}{n^2 + 2} \left(\frac{\varepsilon - 1}{\varepsilon + 2} - \frac{n^2 - 1}{n^2 + 1} \right) \quad (10)$$

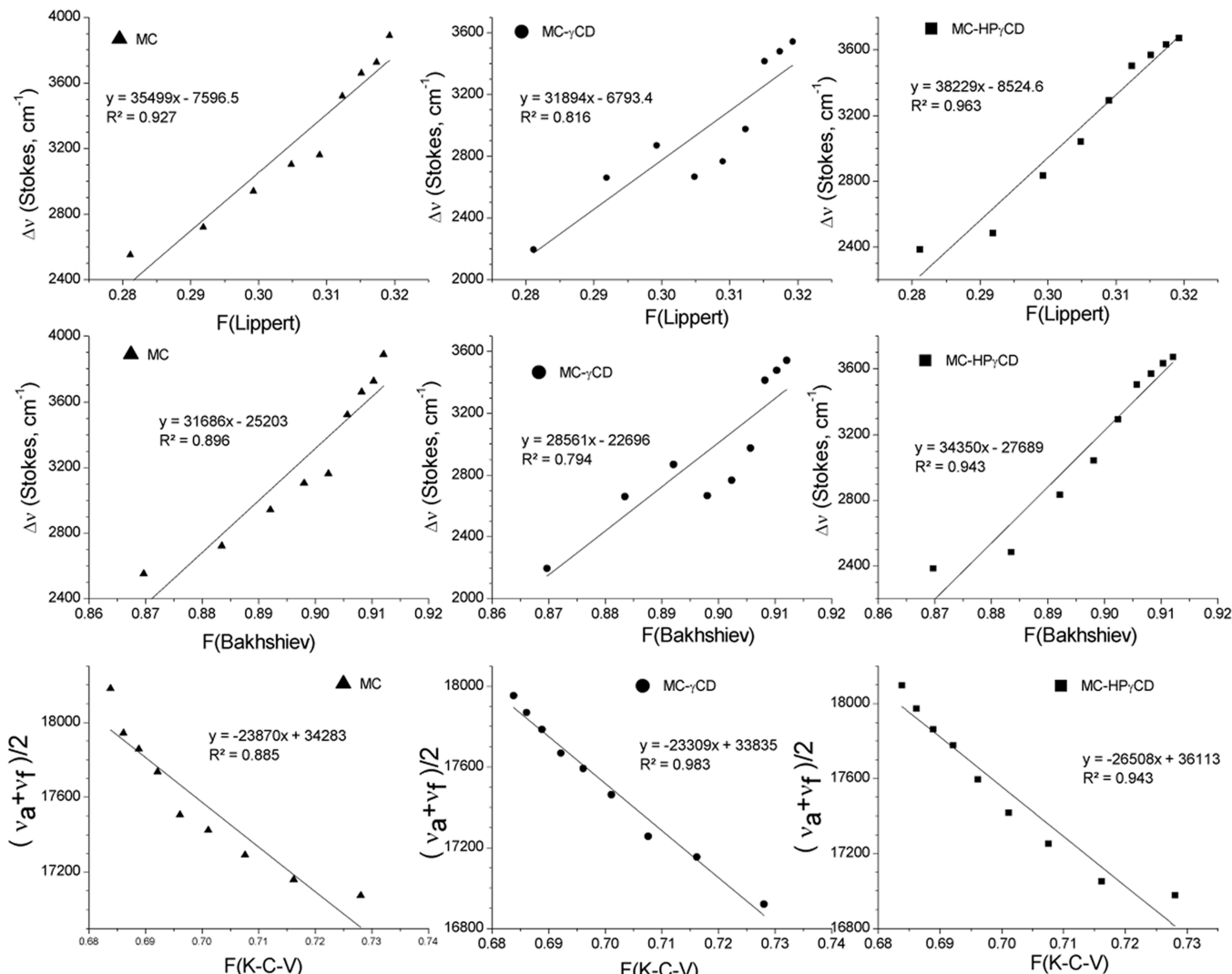


Figure 7. Lippert–Mataga, Bakhshiev, and Kawski–Chamma–Viallet plots of MC, γ CD–MC, and HP γ CD–MC in aqueous–DMSO binary media. The x-axes represent solvent polarity functions, $F(\epsilon, n)$ —orientation polarizability—for each model.

where ϵ is the solvent dielectric constant and n is the refractive index. We used the literature DMSO–water dielectric constants and refractive indices²¹ to determine the polarizability reorientation parameters given in Table 1. The dielectric constant and refractive index have opposite effects on the Stokes shift, the solvent relaxation after photoexcitation.²² An increase in the dielectric constant, which is a static property that depends on electronic and molecular motions, of a medium increases the polarizability reorientation of the fluorophore and the Stokes shift. However, an increase in the refractive index, a property that only depends on the motions of electrons within solvent molecules, of a medium decreases the polarizability reorientation of the fluorophore and hence has the same effect on the Stokes shift. We calculated the cavity radius (a) of merocyanine molecule as 4.29 Å from the estimated spherical molecular volume of 331.15 Å³ obtained from the Spartan '10 v1.0.1 semiempirical PM3 structural optimization. As expected, this value is slightly larger than the Onsager cavity radius of the nitrospiropyran, 4.06 Å, derived from eq 11,

$$a = \left(\frac{3M}{4\pi\delta N} \right) \quad (11)$$

where M is the molecular weight of the solute, δ is the density of the solute (nitrospiropyran = 1.31 g/cm³), and N is Avogadro's number.

The Lippert–Mataga, Bakhshiev, and Kawski–Chamma–Viallet plots of MC, γ CD–MC, and HP γ CD–MC, (Figure 7) as a function of polarizability orientation give information about the change in dipole moment of the molecule upon excitation, $\Delta\mu = \mu_e - \mu_g$. Slopes of the lines, as indicated in Figure 7, are determined by fitting the data to straight line expressions corresponding to eqs 2–4. Applications of expressions 5–7 yield ground and excited state dipole moments. Our results (Table 2) suggest that upon photoexcitation HP γ CD–MC

Table 2. Dipole Moments, in Debye, Experimental in DMSO–Water and Calculated in the Gas Phase

system	μ_g (expt)	μ_e (expt)	$\Delta\mu$ (expt)	μ_g (calc)
MC	18.9	2.7	-16.2	22.3 ^a
	17.7 ^b	11.3 ^b	-6.4 ^b	11.5 ^c
γ CD–MC	17.1	1.7	-15.4	
HP γ CD–MC	19.4	2.5	-16.9	

^aMC in water.²³ ^bMC in dioxane.¹² ^cHF/B3LYP 6-31G* [this work].

experiences the largest dipole moment decrease (16.9 D) while for MC the decrease is 16.2 D and γ CD–MC has the smallest decrease (15.4 D). The measured lower dipole moment for the MC's first excited state compared to the ground state is in accord with theoretical predictions.²³ Moreover, the negative solvatochromism observed in all studied systems also supports the fact that $\mu_e > \mu_g$. The linearity of the Lippert–Mataga, Bakhshiev, and Kawski–Chamma–Viallet plots suggests that general solvent effects are present, due to the interaction of each fluorophore's dipole with its environment. In addition, the observed deviation from linearity for the studied molecules suggests that specific solvent effects resulting from the interaction of the fluorophore with the solvent are also present.

The dependence on solvent polarity of the absorption spectra of MC free and cyclodextrin-bound can potentially be used as a polarity probe, (Figure 8). In comparison, the

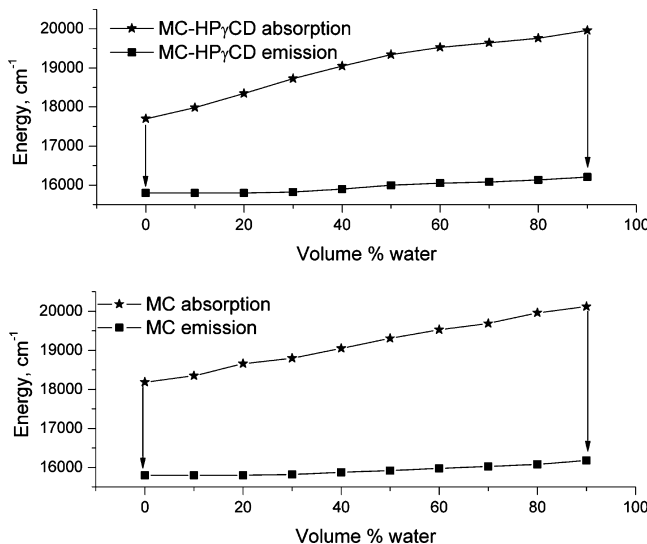


Figure 8. Dependence of the Stokes shifts of HP γ CD–MC and MC on solvent polarity. Binary aqueous–DMSO solutions of higher water content are more polar.

maximum transition energies for fluorescence spectra of the excited state showed a weaker dependence on solvent polarity. This is probably due to a smaller MC dipole moment in the excited state compared to the ground state. The Stokes shifts of the studied molecules scale with the amount of water added to DMSO.

We also measured the fluorescence quantum yields of the solutions (Table 1) using cresyl violet as an internal standard

(reference). The quantum yields of these samples (Q_s) are determined according to the following expression:

$$Q_s = Q_r \frac{I_s A_r n_s^2}{I_r A_s n_r^2} \quad (12)$$

where Q_r is the quantum yield of cresyl violet (ca. 0.54, excitation wavelength 540 nm and emission at 640 nm in methanol);²² I_s is the emission intensity of the sample; I_r is the emission intensity of the reference; A_r is the absorbance of the reference; A_s is the absorbance of the sample; and n_s and n_r are the refractive indices of the sample and reference, respectively. In general, no specific trends were observed for the quantum yields of MC, γ CD–MC, and HP γ CD–MC in aqueous–DMSO binary solvents. However, at higher viscosities ($\eta \geq 3$), the quantum yield scaled with the viscosity of the media. This is an expected observation since in a highly viscous environment the change in conformation of the molecule needed for charge transfer—a nonradiative process—is hindered thus radiative decay is favored.

4. Medium Acidity, Basicity, and Polarity Effects on Absorption and Emission Spectra. Application of the Kamlet–Taft multiparameter model—expression 12—allows the measurement of the sensitivity of the molecular properties to environmental acidity, basicity, and polarizability/polarity.²⁴ We fit the Stokes shifts and absorption and fluorescence maximum energies to the following relationship:

$$P = s\pi^* + a\alpha + b\beta + P_0 \quad (13)$$

where P stands for a molecular property which can be either Stokes shifts, or absorption, or fluorescence maximum energies; π^* , α , and β are solvent parameters that stand respectively for the Kamlet–Taft scales for solvent polarity/polarizability, hydrogen bond donor (acidity), and hydrogen bond acceptor (basicity); s , a , and b are coefficients that measure the susceptibility of the property studied to the solvent parameters; and P_0 is an intercept. Positive coefficients indicate a stabilization of the molecular property whereas negative coefficients show destabilization.

We determined s , a , b , and P_0 by multiple linear regression analysis using Origin 8.0 (Table 3). For the unbound MC, the estimated polarizability (s), acidity (a), and basicity (b) are positive implying that these three solvent parameters effectively stabilize the spectral energies for this system in DMSO–water. The absorption maximum energies are most stabilized possibly due to a large ground state dipole moment. The solvent basicity is the dominant stabilizing parameter, by an order of magnitude in the coefficients,

Table 3. Sensitivity of Stokes' Shifts and Absorption (ν_a) and Fluorescence (ν_f) Maximum Energies to Aqueous DMSO Solvent Polarity/Polarizability, Basicity, and Acidity

system	property	s (polarizability)	b (basicity)	a (acidity)	R^2
MC	ν_a (cm ⁻¹)	2141 ± 1117	10046 ± 6574	5757 ± 2459	0.986
	ν_f (cm ⁻¹)	1232 ± 441	6913 ± 2897	3132 ± 971	0.964
	$\Delta\nu_{\text{Stokes}}$ (cm ⁻¹)	914 ± 1098	3143 ± 6464	2629 ± 2417	0.978
γ CD–MC	ν_a (cm ⁻¹)	3258 ± 1088	-13545 ± 6403	-3202 ± 2394	0.985
	ν_f (cm ⁻¹)	-591 ± 681	-7450 ± 4011	-2349 ± 1500	0.950
	$\Delta\nu_{\text{Stokes}}$ (cm ⁻¹)	3850 ± 1520	-5996 ± 8950	-853 ± 3346	0.940
HP γ CD–MC	ν_a (cm ⁻¹)	-1935 ± 669	7385 ± 3940	4522 ± 1473	0.996
	ν_f (cm ⁻¹)	1245 ± 256	4809 ± 1506	2392 ± 563	0.990
	$\Delta\nu_{\text{Stokes}}$ (cm ⁻¹)	-3180 ± 795	2573 ± 4683	2129 ± 1751	0.990

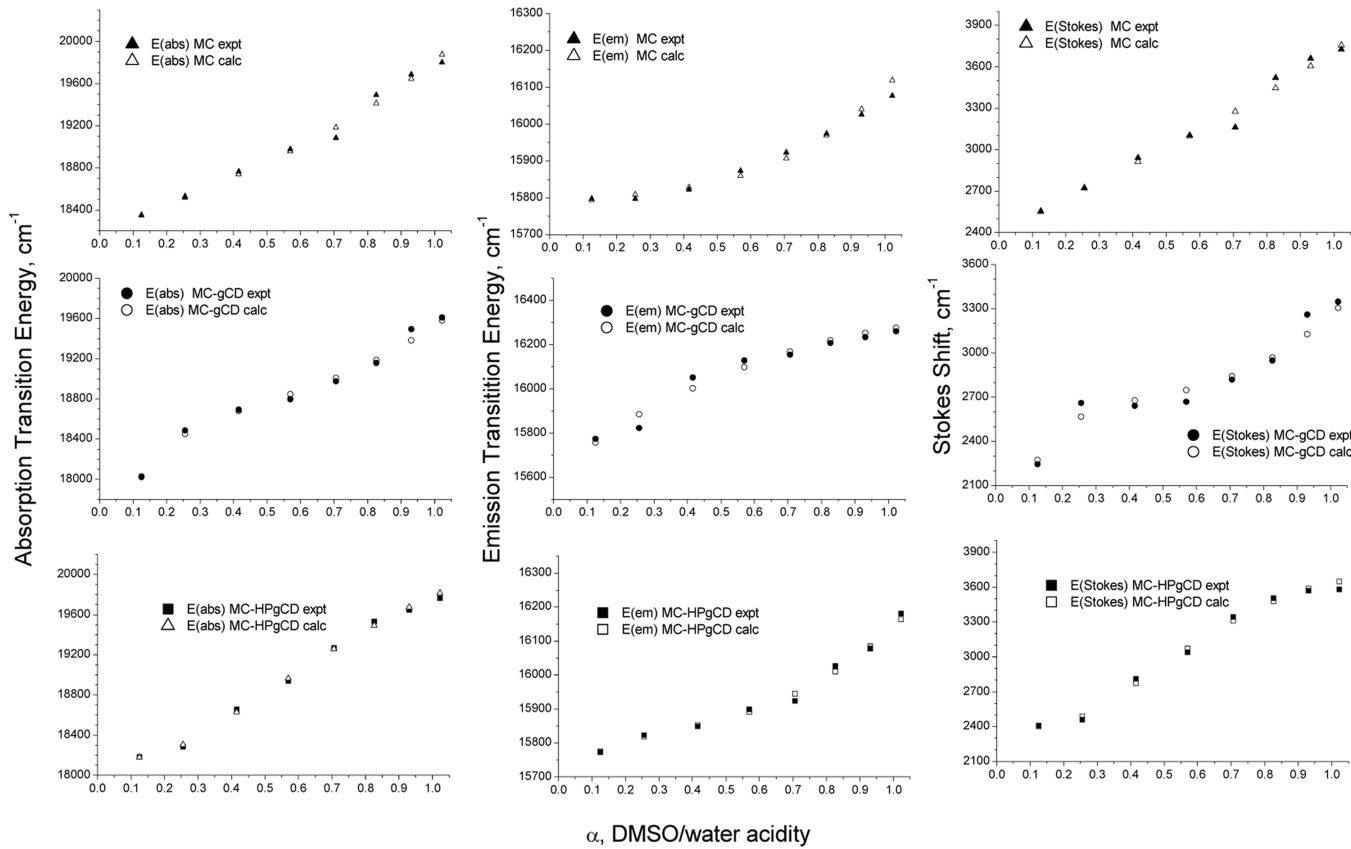


Figure 9. Stokes shifts and absorption and emission maximum energies as a function of volume percent water in DMSO. Comparison between experimental values (filled symbols) and calculated (unfilled symbols) values using the Kamlet-Taft multiparameter model.

followed by the solvent acidity, whereas the solvent polarizability is the least stabilizing factor.

For the γ CD-MC complex (Table 3), the estimated coefficients for the solvent parameters are mostly negative. The magnitude of the estimated coefficients indicates that the solvent polarizability is the most stabilizing parameter, followed by the solvent acidity whereas the solvent basicity is the least stabilizing factor. Interestingly, the observed trend for the estimated coefficients of the γ CD-MC complex is $s > a > b$ whereas the one for unbound MC is $s < a < b$, i.e. the reverse. This may be due to the shielding or encapsulation of merocyanine by the cavity of the γ CD that minimizes solvent interactions between the MC and the DMSO-water.

For the HP γ CD-MC complex (Table 3), the estimated coefficients for the solvent parameters are mostly positive. However, the coefficients for the polarizability parameter for the Stokes shift and absorption maximum transition energy are negative. The order of magnitude of the estimated coefficients indicates that the absorption maximum energies are mostly stabilized by the solvent basicity and acidity whereas the solvent polarizability destabilizes them. The signs of the solvent polarizability coefficients for the HP γ CD-MC are opposite from the ones for the γ CD-MC; this suggests different structural conformations between the two host-guest complexes.

Figure 9 shows a good correlation between experimental (filled symbols) and predicted (open symbols) Kamlet-Taft thermosolvatochromic parameters for the merocyanines, both bound to cyclodextrin and free.

It is noteworthy that the repeated interconversion of spiro-pyran to merocyanine in DMSO-water is stable and does not

suffer thermal or photofatigue (Figure 10). Therefore, the studied systems could potentially be used repeatedly as polarity sensors.

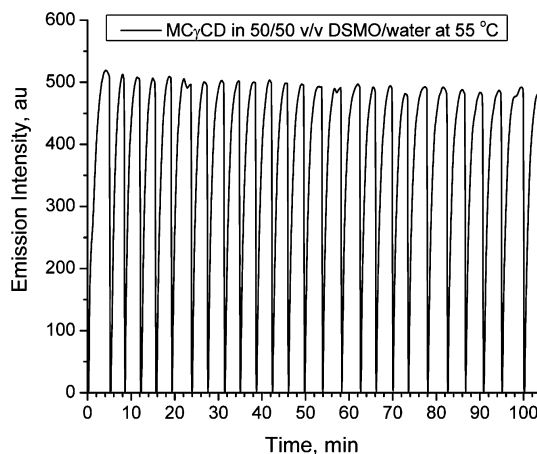


Figure 10. Twenty-six cycles of the interconversion of γ CD-SP to γ CD-MC. SP was converted to MC by heating the sample up to 55 °C then MC was converted back to SP via visible light irradiation from a light emitting diode at approximately every 3 min. The excitation wavelength of γ CD-MC in DMSO-water 50/50 v/v is at 520 nm, and emission is at 640 nm.

CONCLUSIONS

We have measured the thermosolvatochromism of merocyanines free and bound to cyclodextrin in binary DMSO-water

mixtures of increasing polarity. Our results suggest that HP γ CD–MC experiences the largest dipole moment change ($\Delta\mu = 16.9$ D) upon photoexcitation $S_1 \leftarrow S_0$, followed by MC ($\Delta\mu = 16.2$ D). In contrast, γ CD–MC exhibits the smallest change ($\Delta\mu = 15.4$ D). All three systems reveal both general solvent effects and specific solvent effects. In DMSO–water, the studied molecules do not photodegrade; hence, this system is stable and could potentially contribute to the development of polarity and temperature sensors.

■ ASSOCIATED CONTENT

§ Supporting Information

Figures S1–S3. This information is available free of charge via the Internet at <http://pubs.acs.org>.

■ AUTHOR INFORMATION

Corresponding Author

*E-mail: Buthelezi_thandi@wheatoncollege.edu.

■ ACKNOWLEDGMENTS

This work was supported by start-up funds from Wheaton College and the Wheaton Research Partnerships program. We thank Professors Elita Pastra-Landis and Laura Muller for support and helpful discussions.

■ REFERENCES

- (1) Keum, S.; Roh, S.; Kim, S.; Lee, S.; Cho, C.; Kim, S.; Koh, K. *Bull. Korean Chem. Soc.* **2006**, *27*, 187–188.
- (2) Catalán, J.; Díaz, C.; García-Blanco, F. *J. Org. Chem.* **2001**, *66*, 5846–5852.
- (3) Silva, P. L.; Bastos, E. L.; El Seoud, O. A. *J. Phys. Chem. B* **2007**, *111*, 6173–6180.
- (4) Milani, A.; Fadel, N. A.; Brambilla, L.; del Zoppo, M.; Castiglioni, C.; Zerbi, G.; Stradi, R. *J. Raman Spectrosc.* **2009**, *40*, 1110–1116.
- (5) Banerjee, S.; Roy, S.; Bagchi, B. *J. Phys. Chem. B* **2010**, *114*, 12875–12882.
- (6) Yang, L.; Yang, X.; Huang, K.; Jia, G.; Shang, H. *Int. J. Mol. Sci.* **2009**, *10*, 1261–1270.
- (7) El Seoud, O. A. *Pure Appl. Chem.* **2009**, *81*, 697–707.
- (8) Shiraishi, Y.; Miyamoto, R.; Hirai, T. *Org. Lett.* **2009**, *11*, 1571–1574.
- (9) Reichardt, C. *Solvent effects in organic chemistry*; Wiley-VCH: Weinheim, New York, 1979.
- (10) Reichardt, C. *Pure Appl. Chem.* **2004**, *76*, 1903–1919.
- (11) Chibisov, A. K.; Görner, H. *J. Phys. Chem. A* **1997**, *101*, 4305–4312.
- (12) Bletz, M.; Pfeifer-Fukumura, U.; Kolb, U.; Baumann, W. *J. Phys. Chem. A* **2002**, *106*, 2232–2236.
- (13) Wojtyk, J. T. C.; Wasey, A.; Kazmaier, P. M.; Hoz, S.; Buncel, E. *J. Phys. Chem. A* **2000**, *104*, 9046–9055.
- (14) Rodante, F.; Marrosu, G. *Thermochim. Acta* **1988**, *136*, 209–218.
- (15) Lippert, E. Z. *Naturforsch.* **1955**, *10A*, 541–545.
- (16) Mataga, N.; Kaifu, Y.; Koizumi, M. *Bull. Chem. Soc. Jpn.* **1956**, *29*, 465–470.
- (17) Bakhshiev, N. G. *Opt. Spektrosk.* **1964**, *16*, 821–832.
- (18) Kawski, A.; Bilot, L. *Acta Phys. Polon.* **1964**, *26*, 41–45.
- (19) Kawski, A. *Acta Phys. Polon.* **1966**, *29*, 507–518.
- (20) Chamma, A.; Viallet, P. C. *R. Acad. Sci. C* **1970**, *270*, 1901–1904.
- (21) Gayathri, B. R.; Mannekutla, J. R.; Inamdar, S. R. *J. Mol. Struct.* **2008**, *889*, 383–393.
- (22) Lakowicz, J. R. *Principles of Fluorescence Spectroscopy*, 2nd ed.; Kluwer Academic: New York, 1999.
- (23) (a) Murugan, N. A.; Chakrabarti, S. A. *J. Phys. Chem. B* **2011**, *115*, 4025–4032. (b) Cottone, G.; Noto, R.; La Manna, G.; Fornili, S. L. *Chem. Phys. Lett.* **2000**, *319*, 51–59.

- (24) (a) Kamlet, M. J.; Abboud, J.-M.; Abraham, M. H.; Taft, R. W. *J. Org. Chem.* **1983**, *48*, 2877–2887. (b) Laurence, C.; Nicolet, P.; Helbert, M. *J. Chem. Soc. Per. Trans. 2* **1986**, *1081*–1090. (c) Kamlet, M. J.; Abboud, J. L.; Taft, R. W. *J. Am. Chem. Soc.* **1977**, *99*, 6027–6038. (d) Taft, R. W.; Kamlet, M. J. *J. Am. Chem. Soc.* **1976**, *98*, 2886–2894. (e) Rosario, R.; Gust, D.; Hayes, M.; Springer, J.; Garcia, A. A. *Langmuir* **2003**, *19*, 8801–8806.